Published in final edited form as:
Neuroimage. 2012 November 15; 63(3): 1107–1118. doi:10.1016/j.neuroimage.2012.08.042.

Data-driven analysis of analogous brain networks in monkeys and humans during natural vision

Dante Mantini[1,2,3], **Maurizio Corbetta**[2,3,4,5], **Gian Luca Romani**[2,3], **Guy A. Orban**[1,6], and **Wim Vanduffel**[1,7,8]

[1]Laboratory of Neuro- and Psychophysiology, KU Leuven Medical School, Leuven, Belgium

[2]Department of Neuroscience and Imaging, G. D'Annunzio University, Chieti, Italy

[3]Institute for Advanced Biomedical Technology, D'Annunzio University Foundation, Chieti, Italy

[4]Department of Neurology, Washington University, St. Louis, MO, USA

[5]Department of Radiology, Washington University, St. Louis, MO, USA

[6]Department of Neuroscience, University of Parma Medical School, Parma, Italy

[7]Athinoula A. Martinos Center for Biomedical Imaging, Charlestown, MA, USA

[8]Department of Radiology, Harvard Medical School, Boston, MA, USA

Abstract

Inferences about functional correspondences between functional networks of human and non-human primates largely rely on proximity and anatomical expansion models. However, it has been demonstrated that topologically correspondent areas in two species can have different functional properties, suggesting that anatomy-based approaches should be complemented with alternative methods to perform functional comparisons. We have recently shown that comparative analyses based on temporal correlations of sensory-driven fMRI responses can reveal functional correspondent areas in monkeys and humans without relying on spatial assumptions. Inter-species activity correlation (ISAC) analyses require the definition of seed areas in one species to reveal functional correspondences across the cortex of the same and other species. Here we propose an extension of the ISAC method that does not rely on any seed definition, hence a method void of any spatial assumption. Specifically, we apply independent component analysis (ICA) separately to monkey and human data to define species-specific networks of areas with coherent stimulus-related activity. Then, we use a hierarchical cluster analysis to identify ICA-based ISAC clusters of monkey and human networks with similar timecourses. We implemented this approach on fMRI data collected in monkeys and humans during movie watching, a condition that evokes widespread sensory-driven activity throughout large portions of the cortex. Using ICA-based ISAC, we detected seven monkey-human clusters. The timecourses of several clusters showed significant correspondences with either the motion energy in the movie or with eye-movement parameters. Five of the clusters spanned putative homologous functional networks in either primary or extrastriate visual regions, whereas two clusters included higher-level visual areas at topological locations that are not predicted by cortical surface expansion models. Overall, our

Corresponding author: Dr. Wim Vanduffel Athinoula A. Martinos Center for Biomedical Imaging 13th Street, Building 149, Charlestown, MA 02129. Telephone: +1 617 726 0318 Fax: +1 617 726 7422 wim@nmr.mgh.harvard.edu.

ICA-based ISAC analysis complemented the findings of our previous seed-based investigations, and suggested that functional processes can be executed by brain networks in different species that are functionally but not necessarily anatomically correspondent. Overall, our method provides a novel approach to reveal evolution-driven functional changes in the primate brain with no spatial assumptions.

Keywords

cluster analysis; independent component analysis; functional magnetic resonance imaging; primate brain; evolution; functional correspondence

1. Introduction

A number of studies have investigated the functional architecture of macaque and human brains using natural viewing conditions, instead of highly controlled conditions (Bartels et al., 2008; Bartels and Zeki, 2005; Maguire et al., 1998; Moeller et al., 2009; Rolls et al., 2003; Willmore et al., 2010). Interestingly, neural responses evoked with natural stimuli, being more sparse and/or statistically independent than those evoked with artificial stimuli (Felsen and Dan, 2005; Vinje and Gallant, 2000), are widespread, highly reliable and functionally selective throughout the brain (Hasson et al., 2010). Notably, monkeys and humans attend a common set of events during movie watching (Shepherd et al., 2010), which enables us to investigate lower- and higher-level sensory areas that show stimulus-related activity in both species.

Functional magnetic resonance imaging (fMRI) activation patterns in the two primate species are usually studied and interpreted relying on spatial assumptions related to cortical surface expansion. In particular, cortical surface expansion models use putative homologous areas as corresponding landmarks in monkeys and humans to align the fMRI activation maps, and to assess inter-species functional similarities (analogies) across the cortex (Van Essen and Dierker, 2007). By and large, the cortical surface expansion model probably holds true for most of the cortex (Orban et al., 2004; Van Essen et al., 2011a; Van Essen et al., 2011b). A number of comparative fMRI studies, however, have failed in revealing functional correspondences between anatomically corresponding areas (Orban et al., 2006; Vanduffel et al., 2002), suggesting that evolutionary changes in anatomy and function are not necessarily linked. In particular, specific functions may be preserved in areas that anatomically correspond, absent in one of the two primate species, or shifted to other cortical locations. Comparative models with spatial constraints do not allow to distinguish between the latter two possibilities.

To overcome this limitation, hence to assess analogies without imposing topological constraints, we developed a method which allowed us to measure the temporal correlation between sensory-driven fMRI responses for identifying analogies across species (Mantini et al., 2012). According to this seed-based inter-species activity correlation (ISAC) approach, the average timecourse in a selected brain area of one species is correlated to the brain voxels with significantly correlated activity in the other species. To ensure sufficient sensitivity in the correlation analyses, the ISAC method includes specific pre-processing techniques to remove both non-neuronal and non-selective signals shared across multiple brain areas. The detection of analogous networks by the ISAC method still relies on the definition of seed areas. Data-driven analyses, however, may be more promising for large-scale analyses of natural vision data (Bartels and Zeki, 2005; Moeller et al., 2009), because limited information about the timing and order of the stimuli, and on how these relate to the measured brain responses, is available.

For the detection of analogies between species without using predetermined stimulation protocols or prior knowledge about brain area definitions, we propose an extension of the ISAC approach that relies on data-driven analyses. Specifically, we apply independent component analysis (ICA) separately to monkey and human data to define species-specific networks of areas with coherent stimulus-related activity. Then, we use a hierarchical cluster analysis to identify ICA-based ISAC clusters of monkey and human networks with similar timecourses (hence inter-species clusters). To test the applicability of the ICA-based ISAC approach, we apply it to fMRI data collected in monkeys and humans under freeviewing of an original audiovisual feature film (Hasson et al., 2004; Hasson et al., 2010; Mantini et al., 2012).

2. Methods

We used the same fMRI data as in our previous study (Mantini et al., 2012). In the re-analysis presented here, we examined inter-species functional correspondences between cortical networks in monkeys and humans without using regions of interest (ROIs) defined a-priori (Fig. 1). Specifically, we applied ICA separately to monkey and human data to decompose them into independent components (ICs), representing functionally-specific cortical networks. Then, we used hierarchical cluster analysis to define clusters of monkey and human ICs with common temporal responses.

2.1. Subjects

Four rhesus monkeys (macaca mulatta, one female, 4-6 kg, 4-7 years old) and twenty-four right-handed Italian-speaking young healthy volunteers (15 females, 20–31 years old) participated in the study. Animal care procedures met the Belgian and European guidelines, and were approved by the K.U. Leuven Medical School. Human volunteers were informed about the experimental procedures and signed a written informed consent. The study design was approved by the local Ethics Committees of both the KU Leuven and the Chieti University, for experiments in monkeys and humans respectively.

2.2 Data collection

2.2.1 Behavioral task—We carried out a natural vision experiment, in which the subjects watched and listened to 30 minutes of the Italian version of the movie “the Good the Bad and the Ugly” (Hasson et al., 2004), from minute 16:48 to minute 46:48. The movie was divided into 3 clips of 10 minutes each. The movie clips were presented 6 times to the monkeys, and one time to the human subjects.

2.2.2 Experimental setup—Human volunteers lay in a supine position and watched the clips through a mirror tilted 45 degrees towards a translucent screen onto which the movie was projected at a frame rate of 60Hz. The subjects were allowed to watch the movie clips freely while keeping their gaze within the projection area (24×10.2 visual degrees, 640×272 pixels). A similar freeviewing condition was achieved in monkeys by rewarding them with juice when their gaze was kept within the 24 × 10.2 degree virtual window covering the projected movie (Vanduffel et al., 2002). Monkeys were prepared for scanning as in our previous studies (Vanduffel et al., 2001; Vanduffel et al., 2002). In particular, a bolus of microcrystalline-iron-oxide-nanoparticles (MION; Sinerem®, Guerbet; 6-10 mg/kg) was injected into the femoral/saphenous vein of the animal prior to fMRI scanning. For both monkeys and humans, eye position was monitored using a pupil-corneal reflection system at 120 Hz (Iscan, Burlington, MA, USA). Furthermore, MR-compatible headphones with ear-cup pad were used to deliver the acoustic stimuli associated with the movie, and to shield the ears from environmental noise (Joly et al., 2011).

2.2.3 fMRI data acquisition—Monkey fMRI was performed with a 3T MR Siemens Trio scanner in Leuven, Belgium. The functional images were collected using a gradient-echo T2-weighted echo-planar sequence (40 slices, 84 × 84 in-plane matrix, TR/TE=2000/19 ms, flip angle=75°, voxel size=1.25×1.25×1.25 mm^3). In addition, high resolution, T1-weighted anatomical images (MP-RAGE sequence, TR/TE=2200/4.06, voxel size=0.5×0.5×0.5 mm^3) were collected in separate sessions under ketamine-xylazine anesthesia to provide the anatomical reference for the functional scans.

fMRI in humans was performed with a 3T MR Philips Achieva scanner in Chieti, Italy. The functional images were obtained using T2-weighted echo-planar images (EPI) with BOLD contrast using SENSE imaging. EPIs comprised 32 axial slices acquired continuously in ascending order and covering the entire brain (32 slices, 230 × 230 in-plane matrix, TR/TE=2000/35 ms, flip angle=90°, voxel size=2.875×2.875×3.5 mm^3). Furthermore, a three-dimensional high-resolution T1-weighted image was collected by means of an MP-RAGE sequence (TR/TE=8.1/3.7 ms, voxel size=0.938×0.938×1 mm^3).

2.3. Data analysis

2.3.1 Analysis of motion in the movie—We measured the amount of motion contained in the movie clips presented to the subjects, in order to correlate this information with the recorded fMRI signals. The amount of motion within each frame was extracted using the optical flow metric defined by the Lucas-Kanade method (Beauchemin and Barron, 1995; Lucas and Kanade, 1981). Total motion was calculated from motion vectors for each pair of consecutive frames, removing the effect of scene changes by means of automated movie segmentation (Hanjalic et al., 1999).

2.3.2 Eye gaze analysis—We also analyzed eye-movement trajectories obtained during the fMRI scanning. First, we converted eye traces to visual degrees. Saccades were detected as portions of the traces in which the velocity was 3 standard deviations or more above the mean for at least 60 consecutive ms (Joly et al., 2011). For each movie repetition and each subject, we measured the number of saccades per minute (saccade rate), the amount of time with similar (distance < 3 visual degrees) gaze positions (eye-position overlap), the average distance in gaze position with respect to the center of the screen (eye-position variability) (Mantini et al., 2012; Shepherd et al., 2010). Furthermore, we computed the speed in the x- and y-directions of the eye-movements and calculated the square root of the sum of their squares (Shepherd et al., 2010); we used the resulting eye-speed timecourses to calculate the inter-subject correlation of eye gazes (eye-gaze synchronization) for monkeys and humans, separately (Mantini et al., 2012; Shepherd et al., 2010). Finally, we averaged the eye-speed across monkeys and humans, respectively, to generate an eye-speed timecourse for each of the two primate species, and we correlated them to estimate the eye-gaze synchronization between species (Mantini et al., 2012; Shepherd et al., 2010).

2.3.3. fMRI data preprocessing—fMRI data preprocessing was performed with the SPM5.0 software package (Wellcome Trust Centre for Neuroimaging, London, UK). We preprocessed functional time-series to compensate for slice-dependent time shifts, head motion and linear trends. We spatially warped the monkey and human data to F99 and MNI atlas space, respectively. The final spatial resolution was 1 and 3 mm isotropic for the two species, respectively. To reduce the contribution of artifactual sources, we regressed out signals from ROIs centered in the ventricles and the white matter, respectively (Vincent et al., 2007). Next, we spatially smoothed the data with a Gaussian kernel at 1.5 and 4.5 mm FWHM, respectively for monkeys and humans.

We further applied temporal preprocessing to the fMRI data to minimize signal differences arising from the different hemodynamic response functions (HRFs). To compensate for different hemodynamic peak delays and spectral contents, we convolved the monkey and human fMRI timecourses with a canonical human and monkey HRF (Mantini et al., 2012), respectively. To avoid any border effects due to signal convolution, we removed the first 20 and the last 10 functional volumes from each run, and we converted the resulting fMRI timecourses to Z-scores. Next, we averaged them across repetitions of the same movie clip and across individuals (Mantini et al., 2012) to maximize the relative contribution of stimulus-evoked responses over spontaneous activity in our analysis.

The conversion from volumes to surfaces was performed with Caret 5.61 software (http://brainvis.wustl.edu/wiki/index.php/Caret:About) (Van Essen, 2011; Van Essen and Dierker, 2007). The surface maps were visualized on a flattened cortex, together with the borders of visuotopic areas included in the Caret software (Van Essen, 2011). The use of borders was intended to provide a topological reference that can help the comparison of results across research groups.

2.3.4 Detection of species-specific IC-clusters—We separately decomposed the monkey and human fMRI data into patterns of spatially independent activity by means of ICA (Bartels and Zeki, 2005; Esposito et al., 2005), thus identifying sets of voxels in the brain with ‘coherent’ activation profiles (networks). We performed an ICA decomposition of the monkey and human fMRI data, separately for each of the 3 movie clips (corresponding to 270 fMRI volumes). ICs were estimated by means of the FastICA algorithm, with a deflation approach and hyperbolic tangent (*tanh)* non-linearity. For the monkey and the human ICA decompositions, we compared the three IC datasets using the self-organizing clustering ICA (sogICA) method (Esposito et al., 2005). The sogICA method generated clusters containing spatially-consistent ICs across different movie clips. For each species-specific cluster, we assessed the reliability by means of the similarity index, defined as the difference between the average intra- and extra-cluster correlations (Esposito et al., 2005; Himberg et al., 2004). We selected for the inter-species analysis only the IC clusters with complete consistency across movie clips (N=3) and significant difference between intra- and extra-cluster correlations (Mann-Whitney U-test, $P<0.05$). For each of these selected clusters, we temporally concatenated the three constituting ICs for subsequent analyses.

2.3.5 Detection of inter-species IC-clusters—We cross-correlated the monkey and human IC timecourses, and we selected the pairs of ICs with the strongest inter-species similarities. We extracted those ICs from the two original IC datasets (monkey and human), and we applied hierarchical cluster analysis on them, using the correlation-similarity metric and the average linkage function (Everitt et al., 2011). The number of clusters was uniquely defined as the maximum number of clusters containing at least one monkey and one human IC. The cluster timecourses were obtained by averaging the timecourses from the constituent ICs. We calculated the silhouette, a measure of clustering reliability (Everitt et al., 2011), for each of the clusters, which were subsequently sorted in descending order based on this parameter. This procedure yielded, without any spatial constraint, joint monkey-human clusters containing monkey and human ICs with similar activation profiles (as defined by temporal clustering). To assess the homogeneity in the activation profiles of the clustered ICs, we visualized the intra-cluster and inter-cluster similarities in a two-dimensional space using multidimensional scaling (MDS) (Esposito et al., 2005).

2.3.6 Spatial and temporal analysis of inter-species IC-clusters—We analyzed the monkey-human IC clusters both in the spatial and temporal domains. For the spatial analysis, the areas in each IC map were classified on the basis of the available data on

cortical subdivisions, either those of the monkey or the human cortex. For the temporal analysis, we measured the similarities in the IC cluster timecourses with *i)* the average eye-speed across monkey and human subjects, and with *ii)* the amount of motion in the movie. To this end, we convolved the related signals with both the human and monkey HRFs, resampled them to the fMRI temporal resolution and finally, extracted the samples corresponding to the fMRI signals analyzed. Next, we calculated the temporal correlations of the monkey eye-speed, human eye-speed and motion timecourses with each of the IC cluster timecourses.

2.3.7 Comparison of inter-species ICA-based clustering with voxel-based clustering—To validate the inter-species activity correlation results obtained on IC timecourses, we conducted a complimentary data-driven analysis on fMRI timecourses extracted directly from monkey and human areas (Mantini et al., 2012). To ensure the comparability of the results between the two methods, we selected for this second data-driven analysis only these voxels that were included in the monkey and human ICs composing the inter-species IC clusters. Furthermore, we applied hierarchical clustering using the same algorithm settings (correlation-similarity metric and average linkage function), as well as the same number of output clusters as in the ICA-based clustering. After the definition of maps containing monkey and human voxels belonging to the same cluster, we used the spatial overlap between maps resulting from the voxel-based and the ICA-based clustering, respectively. For each pair of cluster maps, the spatial overlap was defined as the ratio between the number of voxels in their intersection and in their union, respectively. Its value therefore ranged between 0 and 1. We measured the spatial overlap values keeping separate the voxels in the monkey and human brain, so that we could evaluate the correspondence of the ICA-based clustering and voxel-based clustering in each of the two species.

3. Results

3.1. Eye gaze analysis

Our analysis of gaze data revealed that monkeys and humans attended a common set of events during movie watching (Table 1). Although the variability in the eye traces and the number of saccades were significantly larger in humans than in monkeys (Mann-Whitney U-test, P=0.0138 and P=0.0329, respectively), the eye-movements were characterized by significant (P<0.001) intra-monkey (r=0.36), intra-human (r=0.25) and inter-species synchronization (r=0.22). Similarities in eye-movements were significantly larger across monkeys than across humans (Mann-Whitney U-test, P=0.0018). Importantly, we found that the gaze positions in the two species were similar (distance smaller than 3 visual degrees) for a significant fraction (55.7%) of the total movie duration.

3.2. ICA on monkey and human neuroimaging data

We first analyzed the consistency of the ICA results within the same species, using the three distinct movie clips. In many cases, ICs related to different movie clips were spatially correspondent. For instance, we detected three monkey ICs, one for each movie clip, with corresponding spatial maps largely including the middle temporal area (monkey MT) (Fig. 2A). These ICs were automatically clustered together by means of the sogICA method. We found a similar result for humans ICs with corresponding spatial maps showing the middle temporal complex (MT+), which contains the putative homologue of the monkey MT area (Fig. 2B).

We evaluated statistically the IC clustering across the three movie clips for monkeys and humans, respectively. To this end, we measured the number of ICs in each species-specific

cluster, ranging between 1 and 3, and the similarity index of the cluster itself (Fig. 3A-B). The analysis of spatial correlations within an IC cluster (intra-cluster correlations), compared to the spatial correlations between ICs in a cluster and all other ICs (extra-cluster correlations), allowed us to define reliable ICs to be used in the inter-species analyses (see green bars in Fig. 3C-D). Our ICA-based approach yielded 60 monkey and 73 human IC species-specific clusters characterized by complete consistency across movie clips (N =3) and significant difference between intra- and extra-cluster correlations (Mann-Whitney U-test, $P<0.05$). The monkey ICs selected on the basis of the criteria above largely mapped on primary and higher-order visual areas in the occipital, superior temporal, and frontal regions, and did not include the auditory cortex (Fig. 4A-B). The selected humans ICs mostly encompassed occipital, superior parietal and temporal areas, with largest consistency in primary visual and auditory areas (Fig. 4C). Overall, the consistent ICs covered 11.3% and 18.2% of the monkey and human cortex, respectively.

3.3. inter-species ICA clusters

Since the ICs in the selected species-specific clusters were fully consistent across movie clips (N=3), we concatenated their timecourses for subsequent inter-species analyses. We cross-correlated the timecourses of the 60 monkey and 73 human ICs to assess the presence of significant similarities in functional responses between species. We thresholded the correlation matrix at different levels, resulting in the detection of different clusters with monkey and human ICs. With thresholds ranging between 0.3 and 0.6, the number of inter-species clusters varied between 1 and 7 (Fig. 5). For instance, with $r=0.32$ (FDR of $q=0.01$) a single cluster with 19 monkey and 33 human ICs was defined from our data. The maximum number of clusters was found at $r=0.39$ (FDR of $q=0.001$). With this threshold, 7 monkey and 14 human ICs were retained. In contrast, by setting the threshold to $r=0.44$ (FDR of $q=0.0001$) we selected less ICs (3 monkey and 7 human) for the cluster analysis, so that we obtained only 3 monkey-human clusters.

On the basis of the results described above, we selected a correlation threshold of $r=0.39$ to maximize the number of inter-species clusters, hence to optimize the sensitivity of our inter-species investigations. A detailed analysis of the clustering results (Fig. 6) showed that each of the 7 inter-species clusters were composed of only one monkey IC and a variable number of human ICs (Fig. 6D-E). In particular, clusters 1, 3, 4 and 5 contained one human IC, respectively; cluster 7 included 2 humans ICs; finally, clusters 2 and 6 contained 4 human ICs. Furthermore, the latter two clusters were significantly anti-correlated ($r=-0.59$, $P<0.001$) whereas the timecourses of the other clusters showed completely distinct functional signatures (average correlation $r=0.12$, $P=0.197$) (Fig. 6E-F and 7A). This result was also confirmed by an MDS analysis conducted on the cluster timecourses (Fig. 6F). Importantly, we replicated the clustering results described above by using only the fraction of data corresponding to periods with inter-species similarities in the eye gaze position (Supplementary Fig. 1). Overall, this data selection did not yield substantial changes in the structure in the cross-correlation matrix compared to the one obtained from the whole timecourses (spatial correlation $r=0.955$) (Supplementary Fig. 1A). Furthermore, the same monkey and human ICs passed the threshold set for the inter-species analysis (Supplementary Fig. 1B), as well as the same clusters were delineated by the hierarchical clustering (Supplementary Fig. 1C-D).

Given the data-driven nature of the ICA-based approach, we used the inter-species cluster timecourses to test the functional selectivity of natural-vision responses in monkeys and humans in an unbiased manner. We correlated their timecourse (Fig. 7A) with the optic flow in the movie (i.e. movie motion), and separately with the velocity of the eye movements. The most robust IC cluster (cluster 1) revealed a highly significant correlation ($P<0.001$) with the optic flow in the movie, but also with the eye movements (Table 2). Among other

inter-species clusters, weaker but nonetheless significant ($P<0.01$) correlations were observed either with movie motion (clusters 3, 4 and 7) or eye movements (cluster 6). We did not observe significant correlations between movie motion or the speed of eye movements and the timecourses of clusters 2 and 5. Obviously, the latter timecourses may be correlated with stimulus parameters that have not been assessed in the present study.

As a further analysis, we examined the spatial maps of the monkey and human ICs in each cluster in flattened cortical representations, and we labeled the areas in the monkey and human networks using atlas-based cortical parcellations (Fig. 7B-H). Since we did not conduct retinotopic mapping in our subjects and we therefore could not derive group-specific probabilistic maps of visuotopic areas, the labels should be considered as best estimates. It should be noted that the exact areal definitions are not critical for the interpretation of the current results but are only intended for making comparisons with published atlases. The flat map analysis showed that monkey MT and human MT+ belonged together to cluster 1; cluster 2 included primarily PITd and V4 in the monkey as well as the lateral occipital area 2 (LO-2), the lateral occipital complex (LOC), the middle and posterior STS in the human; clusters 3, 4 and 5 contained topologically-corresponding visual areas (mainly V1/V2/V3) in the two species; cluster 6 contained monkey V3A and a region in the human ventral occipital cortex including V4, but also neighboring areas; finally, cluster 7 was composed of dorsal visual areas (V1 and V3) in the monkey, but both dorsal and ventral areas (V1/V2/V3) in the human.

We validated the ICA-based functional correspondences between monkey and human brain areas by means of a complimentary model-free analysis, based on direct clustering of voxel timecourses (Supplementary Fig. 2). To this end, we selected all the voxels in any of the ICs belonging to the inter-species ICA-base clusters, and we applied hierarchical clustering on the fMRI timecourses from all these voxels. By defining seven clusters on the resulting dendrogram, we could directly compare the spatial overlap between the maps obtained by the ICA-based (Fig. 7B-H) and voxel-based clustering approaches (Fig. 8A), respectively. This comparison showed that the two data-driven methods yielded similar results in terms of functional correspondences between monkey and human areas. Since cluster analysis is a data-driven method, the labeling of the most similar clusters resulting from the two approaches did not match (Fig. 8B). However, for each ICA-based cluster we could observe, consistently in monkeys and in humans, a single voxel-based cluster with very high (>85%) spatial overlap.

4. Discussion

During recent decades, the non-human primate visual system has been used as a model for the human visual system (Orban et al., 2004; Sereno and Tootell, 2005), assuming that similar functions and thus computations are carried out by anatomically corresponding cortical networks (Striedter, 2002). Although this assumption probably holds true for large extents of the cortex, previous studies have demonstrated that, in some cases, functions have been lost or have shifted during evolution to different cortical regions (Anderson, 2010; Dehaene and Cohen, 2007). Recently, we have introduced an inter-species activity correlation (ISAC) method to study analogies between species without using spatial constraints on the cortical surface (Mantini et al., 2012). However, this approach requires the definition of seed areas to reveal analogies across the cortex. In this regard, a coarse definition of brain areas may hinder potential inter-species functional similarities; conversely, the use of a very fine parcellation may not be viable, because in this case the spatial blurring of the fMRI signal may produce overlapping ISAC maps from neighboring seeds. As a complementary approach to our previous study (Mantini et al., 2012), we

proposed here an entirely data-driven approach that combines ICA and cluster analysis to define analogies independently of seed definitions.

4.1. ICA on natural vision data

The dynamic complexity of natural vision induces stimulus-related activity in large portions of the cortex, with brain areas responding selectively to classes of stimuli (Hasson et al., 2004; Hasson et al., 2010). Independent component analysis (ICA) of fMRI data is a data-driven approach to identify and segregate networks of brain areas with highly correlated activity (Calhoun et al., 2001; McKeown et al., 1998). Since freeviewing experiments do not permit the creation of accurate models of task-related responses, ICA can be particularly useful compared to other approaches to reveal functionally specific networks from natural vision data (Bartels and Zeki, 2005; Moeller et al., 2009).

To assess the robustness of the ICA results on our monkey and human fMRI data, we performed IC decompositions separately for each of the three movie clips and we applied the self-organizing ICA (sogICA) approach developed by Esposito et al. (2005). As the sogICA method uses the spatial correlation as similarity metric, we clustered ICs with corresponding maps across different movie clips, without making any assumption on the IC timecourses. Furthermore, we derived by sogICA detailed statistics on the intra- and extra-cluster correlations, which were used to select monkey and human ICs for inter-species comparisons. Importantly, this selection would have been impossible with alternative ICA approaches using concatenated fMRI datasets (Calhoun et al., 2001).

4.2. Clustering of monkey and human ICs

We applied a hierarchical cluster analysis on IC timecourses of monkeys and humans, assuming that ICs reflect coherent activity in specific brain networks and that this activity is driven by the same stimuli in the two species. Therefore we delineated clusters of functionally-selective monkey-human networks with similar stimulus-driven responses, which are overall consistent with previous reports (Nakahara et al., 2002; Orban et al., 2004; Pinsk et al., 2009; Sereno and Tootell, 2005; Tootell et al., 2003; Vanduffel et al., 2002). We found complementary but converging results with respect to those of the seed-based ISAC method (Mantini et al., 2012).

Our analysis yielded clusters of analogous networks in the two species, as expected, clearly extending over a large number of visual regions. Some clusters contained monkey and human networks spanning topologically correspondent cortical regions, either in primary or higher-order visual areas. For example, a cluster contained left V1d/V2d in both monkeys and humans. Another one largely included bilateral monkey MT and human MT+ (Kolster et al., 2009; Kolster et al., 2010; Malikovic et al., 2007; Tootell and Taylor, 1995; Ungerleider and Desimone, 1986). Other clusters contain monkey and human extrastriate visual areas for which little is known about their common functional signatures. Those ICA-based clusters provide specific targets for future comparative investigations.

Overall, the results of our data-driven approach may suggest that the primate brain has undergone a partial reorganization across evolution through which some functionality is executed by presumptively homologous areas but some functions may be shifted to completely unexpected regions that are not anatomically corresponding in the two species. For instance, a monkey network composed of visual areas PITd and V4 was found to be analogous to a distributed human network including LO-2 and LOC, as well as middle and posterior STS. This result does not fit necessarily with the topographical pattern predicted by cortical expansion models, but with an evolutionary-driven functional reorganization of the ventral extrastriate cortex. Also, specific functions of monkey V3A may be shifted to

ventral occipital areas (mainly V4 and surrounding areas) in the human (Mantini et al., 2012). This would be in line with functional differences between the anatomically corresponding monkey V3A and human V3A, observed in relation to motion sensitivity, three-dimensional structure-from-motion and shape sensitivity (Denys et al., 2004; Vanduffel et al., 2002). Alternatively, the similarity in the response profile of monkey V3A and ventral occipital areas may not relate to shifts of function between cortical areas, but be due to particular epochs of the movie that reliably lead to species-specific patterns of fixation. It is indeed possible that monkeys, during these epochs, tend to fixate toward the top of the screen more than humans (placing more stimuli in the lower visual field) and/or humans notice particular objects during these epochs that the monkeys do not notice (due to their more conceptually-driven fixations). The amount of variance unexplained in the analyses of monkey and human fixations (see Table 1) would fit with this possibility.

4.3. Limitations

Our data-driven method for revealing analogies between species provides a complementary approach for comparative fMRI studies, but it has also its limitations. First, it is nearly impossible to have an experimental paradigm in which the internal state of monkeys and humans are completely equal. In comparative fMRI studies, differences in neural responses could be caused by different perceptual and cognitive abilities of monkeys compared to humans and by differences in top-down processing during the experimental task. In this study, we used natural vision data to examine large-scale functional similarities without assuming that individuals in the two species engage the same psychological processes. In particular, our results showed analogies between monkey and human networks spanning a large number of lower- and higher-level sensory areas, which are strongly driven in both species by the powerful multi-modal sensory stimuli. Obviously, monkeys and humans may perceive the movie quite differently. Dedicated comparative experiments using highly-controlled stimuli may be used in future studies to compare functional similarities and differences in specific higher-order functions. Second, multiple channels of information may be concurrently present, potentially limiting the detection of monkey and human networks with similar activation profiles. To address this problem, we have used long movie clips to reduce the probability of stimulus co-occurrence and we have used the consistency across three movie clips as criterion for selecting reliable functional networks. Furthermore, we have optimized our method to detect the configuration with maximum sensitivity (see Fig. 5). Given the aforementioned limitations, the current data should be interpreted with caution: although unlikely, the shifts in functionality to anatomically unpredicted locations could possibly reflect differences in the functions engaged during natural vision.

5. Conclusion

Our analysis showed the attractive power of natural vision to evoke similar activations in specific networks of low- and higher-level sensory areas in the two species. Furthermore, it suggested that functional processes are executed in two species by brain networks that are typically but not necessarily anatomically correspondent. Overall, our data-driven description of monkey and human cortical networks with similar responses during natural vision contributes to new frameworks aimed to evaluate in a more unbiased manner evolutionary changes in the functional architecture of the primate brain. Future investigations will be crucial to reveal specific functions that may drive similar responses in putatively analogous networks of different primate species.

Supplementary Material

Refer to Web version on PubMed Central for supplementary material.

Acknowledgments

We thank C. Fransen, C. Van Eupen and A. Coeman for animal training and care; J.T. Arsenault, K. Nelissen, O. Joly, H. Kolster, W. Depuydt, G. Meulemans, P. Kayenbergh, M. De Paep, M. Docx, and I. Puttemans for technical assistance. This work received support from European Union Seventh Framework Programme FWP-200728, Belgian Inter-University Attraction Pole 7/21, Programme Financing PFV/10/008, Geconcerteerde Onderzoeks Actie 10/19, Impulsfinanciering Zware Apparatuur and Hercules funding of the Katholieke Universiteit Leuven, Fonds Wetenschappelijk Onderzoek–Vlaanderen G062208N10, G083111N10 and G043912N, National Science Foundation BCS-0745436 and Geneeskundige Stichting Koningin Elisabeth prize “Janine en Jacques Delaruelle”. D.M. is postdoctoral fellow of the Fonds Wetenschappelijk Onderzoek–Vlaanderen. The Martinos Center for Biomedical Imaging is supported by National Center for Research Resources grant P41RR14075.

Abbreviations

FDR	false discovery rate
fMRI	functional magnetic resonance imaging
HRF	hemodynamic response function
IC	independent component
ICA	independent component analysis
ISAC	inter-species activity correlation
LO-2	lateral occipital area 2
LOC	lateral occipital complex
MT	middle temporal area
MT+	middle temporal complex
PIT	posterior inferotemporal area
ROI	region of interest
sogICA	self-organizing group ICA
STS	superior temporal sulcus

References

Anderson ML. Neural reuse: a fundamental organizational principle of the brain. Behav.Brain Sci. 2010; 33:245–266. [PubMed: 20964882]

Bartels A, Zeki S. The chronoarchitecture of the cerebral cortex. Philos.Trans.R.Soc.Lond B Biol.Sci. 2005; 360:733–750. [PubMed: 15937010]

Bartels A, Zeki S, Logothetis NK. Natural vision reveals regional specialization to local motion and to contrast-invariant, global flow in the human brain. Cereb.Cortex. 2008; 18:705–717. [PubMed: 17615246]

Beauchemin SS, Barron JL. The computation of optical flow. ACM Computing Surveys (CSUR). 1995; 27:433–466.

Calhoun VD, Adali T, Pearlson GD, Pekar JJ. A method for making group inferences from functional MRI data using independent component analysis. Hum.Brain Mapp. 2001; 14:140–151. [PubMed: 11559959]

Dehaene S, Cohen L. Cultural recycling of cortical maps. Neuron. 2007; 56:384–398. [PubMed: 17964253]

Denys K, Vanduffel W, Fize D, Nelissen K, Peuskens H, Van ED, Orban GA. The processing of visual shape in the cerebral cortex of human and nonhuman primates: a functional magnetic resonance imaging study. J.Neurosci. 2004; 24:2551–2565. [PubMed: 15014131]

Esposito F, Scarabino T, Hyvarinen A, Himberg J, Formisano E, Comani S, Tedeschi G, Goebel R, Seifritz E, Di SF. Independent component analysis of fMRI group studies by self-organizing clustering. Neuroimage. 2005; 25:193–205. [PubMed: 15734355]

Everitt, BS.; Landau, S.; Leese, M.; Stahl, D. Cluster Analysis. John Wiley & Sons; London: 2011.

Felsen G, Dan Y. A natural approach to studying vision. Nat.Neurosci. 2005; 8:1643–1646. [PubMed: 16306891]

Hanjalic A, Lagendijk RL, Biemond J. Automated high-level movie segmentation for advanced video-retrieval systems. Ieee Transactions on Circuits and Systems for Video Technology. 1999; 9:580–588.

Hasson U, Malach R, Heeger DJ. Reliability of cortical activity during natural stimulation. Trends Cogn Sci. 2010; 14:40–48. [PubMed: 20004608]

Hasson U, Nir Y, Levy I, Fuhrmann G, Malach R. Intersubject synchronization of cortical activity during natural vision. Science. 2004; 303:1634–1640. [PubMed: 15016991]

Himberg J, Hyvarinen A, Esposito F. Validating the independent components of neuroimaging time series via clustering and visualization. Neuroimage. 2004; 22:1214–1222. [PubMed: 15219593]

Joly O, Ramus F, Pressnitzer D, Vanduffel W, Orban GA. Interhemispheric Differences in Auditory Processing Revealed by fMRI in Awake Rhesus Monkeys. Cereb.Cortex. 2011

Kolster H, Mandeville JB, Arsenault JT, Ekstrom LB, Wald LL, Vanduffel W. Visual field map clusters in macaque extrastriate visual cortex. J.Neurosci. 2009; 29:7031–7039. [PubMed: 19474330]

Kolster H, Peeters R, Orban GA. The retinotopic organization of the human middle temporal area MT/V5 and its cortical neighbors. J.Neurosci. 2010; 30:9801–9820. [PubMed: 20660263]

Lucas, BD.; Kanade, T. An Iterative Image Registration Technique with an Application to Stereo Vision. Proceedings of the 7th International Joint Conference on Artificial Intelligence; 1981. p. 674-679.

Maguire EA, Burgess N, Donnett JG, Frackowiak RS, Frith CD, O'Keefe J. Knowing where and getting there: a human navigation network. Science. 1998; 280:921–924. [PubMed: 9572740]

Malikovic A, Amunts K, Schleicher A, Mohlberg H, Eickhoff SB, Wilms M, Palomero-Gallagher N, Armstrong E, Zilles K. Cytoarchitectonic analysis of the human extrastriate cortex in the region of V5/MT+: a probabilistic, stereotaxic map of area hOc5. Cereb.Cortex. 2007; 17:562–574. [PubMed: 16603710]

Mantini D, Hasson U, Betti V, Perrucci MG, Romani GL, Corbetta M, Orban GA, Vanduffel W. Interspecies activity correlations reveal functional correspondence between monkey and human brain areas. Nat Methods. 2012; 9:277–282. [PubMed: 22306809]

McKeown MJ, Makeig S, Brown GG, Jung TP, Kindermann SS, Bell AJ, Sejnowski TJ. Analysis of fMRI data by blind separation into independent spatial components. Hum.Brain Mapp. 1998; 6:160–188. [PubMed: 9673671]

Moeller S, Nallasamy N, Tsao DY, Freiwald WA. Functional connectivity of the macaque brain across stimulus and arousal states. J.Neurosci. 2009; 29:5897–5909. [PubMed: 19420256]

Nakahara K, Hayashi T, Konishi S, Miyashita Y. Functional MRI of macaque monkeys performing a cognitive set-shifting task. Science. 2002; 295:1532–1536. [PubMed: 11859197]

Orban GA, Claeys K, Nelissen K, Smans R, Sunaert S, Todd JT, Wardak C, Durand JB, Vanduffel W. Mapping the parietal cortex of human and non-human primates. Neuropsychologia. 2006; 44:2647–2667. [PubMed: 16343560]

Orban GA, Van Essen D, Vanduffel W. Comparative mapping of higher visual areas in monkeys and humans. Trends Cogn Sci. 2004; 8:315–324. [PubMed: 15242691]

Pinsk MA, Arcaro M, Weiner KS, Kalkus JF, Inati SJ, Gross CG, Kastner S. Neural representations of faces and body parts in macaque and human cortex: a comparative FMRI study. J.Neurophysiol. 2009; 101:2581–2600. [PubMed: 19225169]

Rolls ET, Aggelopoulos NC, Zheng F. The receptive fields of inferior temporal cortex neurons in natural scenes. J.Neurosci. 2003; 23:339–348. [PubMed: 12514233]

Sereno MI, Tootell RB. From monkeys to humans: what do we now know about brain homologies? Curr.Opin.Neurobiol. 2005; 15:135–144. [PubMed: 15831394]

Shepherd SV, Steckenfinger SA, Hasson U, Ghazanfar AA. Human-monkey gaze correlations reveal convergent and divergent patterns of movie viewing. Curr.Biol. 2010; 20:649–656. [PubMed: 20303267]

Striedter GF. Brain homology and function: an uneasy alliance. Brain Res.Bull. 2002; 57:239–242. [PubMed: 11922967]

Tootell RB, Taylor JB. Anatomical evidence for MT and additional cortical visual areas in humans. Cereb.Cortex. 1995; 5:39–55. [PubMed: 7719129]

Tootell RB, Tsao D, Vanduffel W. Neuroimaging weighs in: humans meet macaques in “primate” visual cortex. J.Neurosci. 2003; 23:3981–3989. [PubMed: 12764082]

Ungerleider LG, Desimone R. Cortical connections of visual area MT in the macaque. J.Comp Neurol. 1986; 248:190–222. [PubMed: 3722458]

Van Essen DC. Cortical cartography and Caret software. Neuroimage. 2011

Van Essen DC, Dierker DL. Surface-based and probabilistic atlases of primate cerebral cortex. Neuron. 2007; 56:209–225. [PubMed: 17964241]

Van Essen DC, Glasser MF, Dierker DL, Harwell J. Cortical Parcellations of the Macaque Monkey Analyzed on Surface-Based Atlases. Cereb.Cortex. 2011a

Van Essen DC, Glasser MF, Dierker DL, Harwell J, Coalson T. Parcellations and Hemispheric Asymmetries of Human Cerebral Cortex Analyzed on Surface-Based Atlases. Cereb.Cortex. 2011b

Vanduffel W, Fize D, Mandeville JB, Nelissen K, Van HP, Rosen BR, Tootell RB, Orban GA. Visual motion processing investigated using contrast agent-enhanced fMRI in awake behaving monkeys. Neuron. 2001; 32:565–577. [PubMed: 11719199]

Vanduffel W, Fize D, Peuskens H, Denys K, Sunaert S, Todd JT, Orban GA. Extracting 3D from motion: differences in human and monkey intraparietal cortex. Science. 2002; 298:413–415. [PubMed: 12376701]

Vincent JL, Patel GH, Fox MD, Snyder AZ, Baker JT, Van E, Zempel JM, Snyder LH, Corbetta M, Raichle ME. Intrinsic functional architecture in the anaesthetized monkey brain. Nature. 2007; 447:83–86. [PubMed: 17476267]

Vinje WE, Gallant JL. Sparse coding and decorrelation in primary visual cortex during natural vision. Science. 2000; 287:1273–1276. [PubMed: 10678835]

Willmore BD, Prenger RJ, Gallant JL. Neural representation of natural images in visual area V2. J.Neurosci. 2010; 30:2102–2114. [PubMed: 20147538]

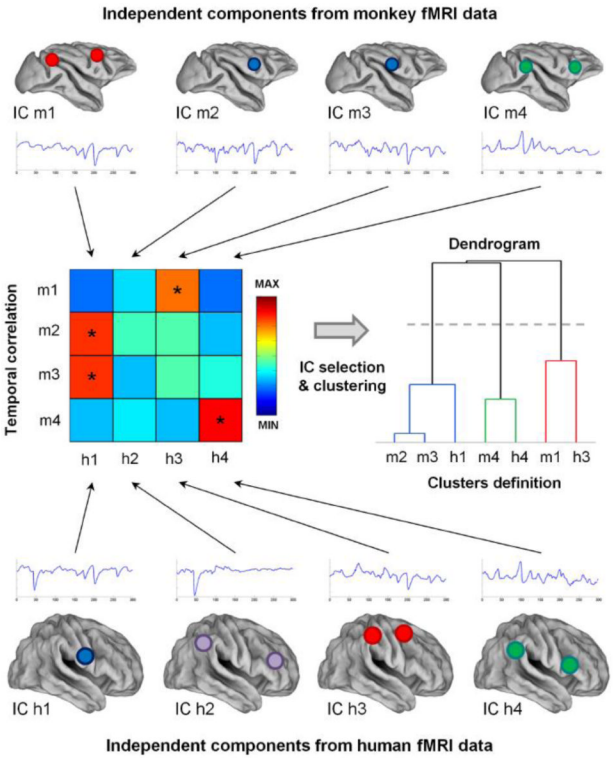

Figure 1. Data-driven analysis of monkey-human functional correspondences

The schematic representation illustrates the analysis pipeline for detecting monkey and human independent components with similar functional processing. First, independent component analysis is used separately on the monkey and human fMRI data. The timecourses of the resulting independent components (ICs) in monkeys and humans are compared by Pearson's correlation. The ICs with at least one significant inter-species correlation are selected for hierarchical cluster analysis. The resulting dendrogram is cut to include at least one monkey and one human IC (see dashed line).

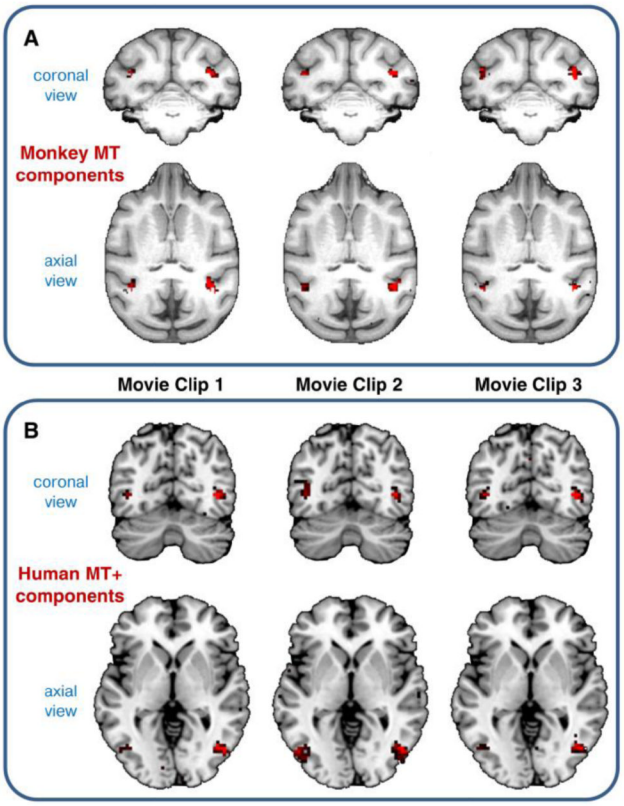

Figure 2. Example of monkey and human ICs detected for different movie clips

Corresponding ICs from the three movie clips are clustered together by means of the sogICA approach. (**A**) Three monkey ICs mainly including the middle temporal area (monkey MT). (**B**) Three human ICs mainly including the middle temporal complex (human MT+). IC spatial maps are thresholded at Z>2 for visualization purposes.

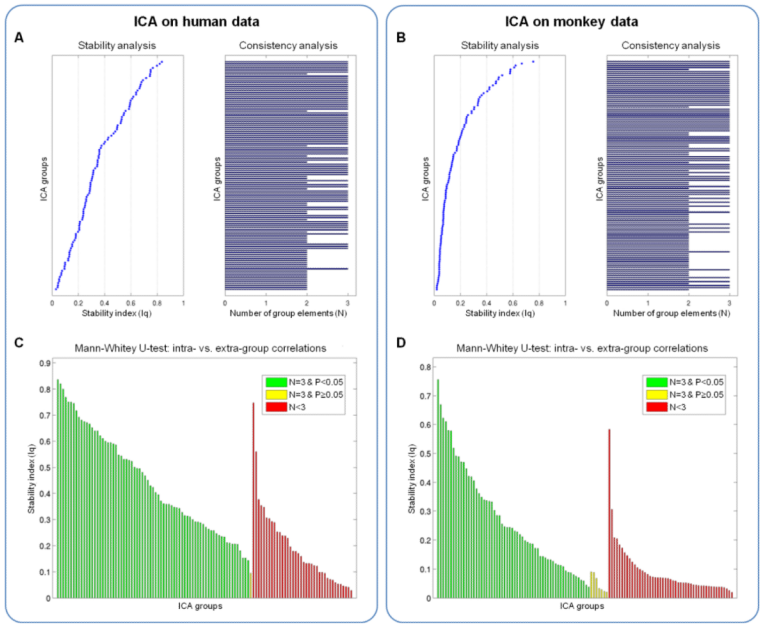

Figure 3. Analysis of ICA clusters from monkey and human data

ICA decomposition was performed on monkey and human data, separately for each of the three movie clips. Spatial cluster analysis was performed, based on the self-organizing group ICA (sogICA) approach, to match corresponding ICs. Stability and consistency were assessed for all (**A**) monkey and (**B**) human ICA clusters. We measured the cluster stability as the difference between intra- and extra-cluster correlations, and the cluster consistency by the number of cluster elements ($N \leq 3$). For inter-species comparisons, we selected the (**C**) monkey and (**D**) human ICA clusters with full consistency across movie clips (N=3) and with significant difference between intra- and extra-cluster correlations (Mann-Whitney U-test, $P<0.05$). The selected ICA clusters are colored in green.

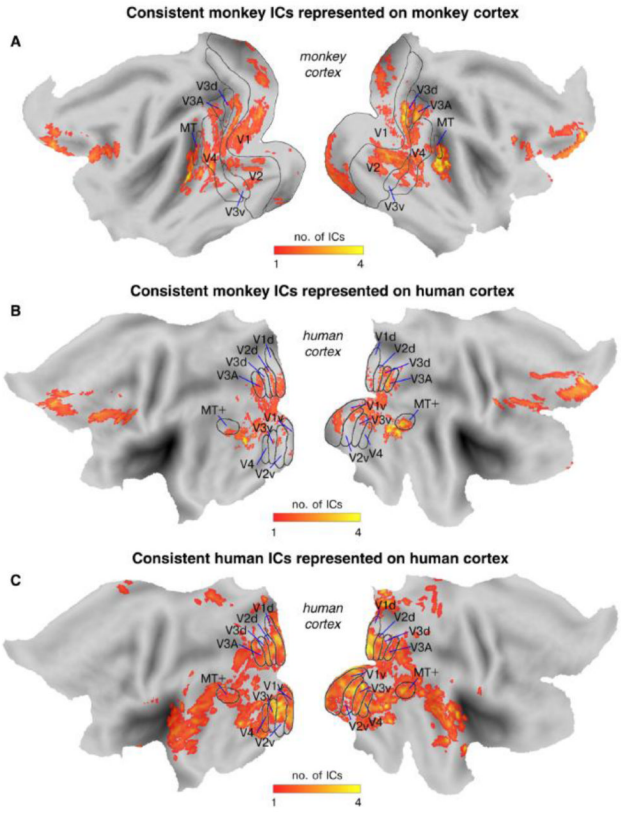

Figure 4. Consistent monkey and human ICs revealed by the species-specific clustering

The spatial maps show the cortical coverage of monkey and human ICs with full consistency across movie clips (N=3) and significant difference between intra- and extra-cluster correlations (Mann-Whitney U-test, $P<0.05$), as reported in Figure 3. The ICs are thresholded at $Z>2$, binarized and summed to generate consistency maps. Boundaries of visuotopic areas are superimposed over the cortex. (**A**) The consistency map for monkey ICs is shown over a representative monkey cortex. (**B**) The same consistency map for monkey ICs is shown over a representative human cortex, by using a computational model for monkey-to-human cortical alignment (Van Essen and Dierker, 2007). (**C**) The consistency map for human ICs is shown over a representative human cortex.

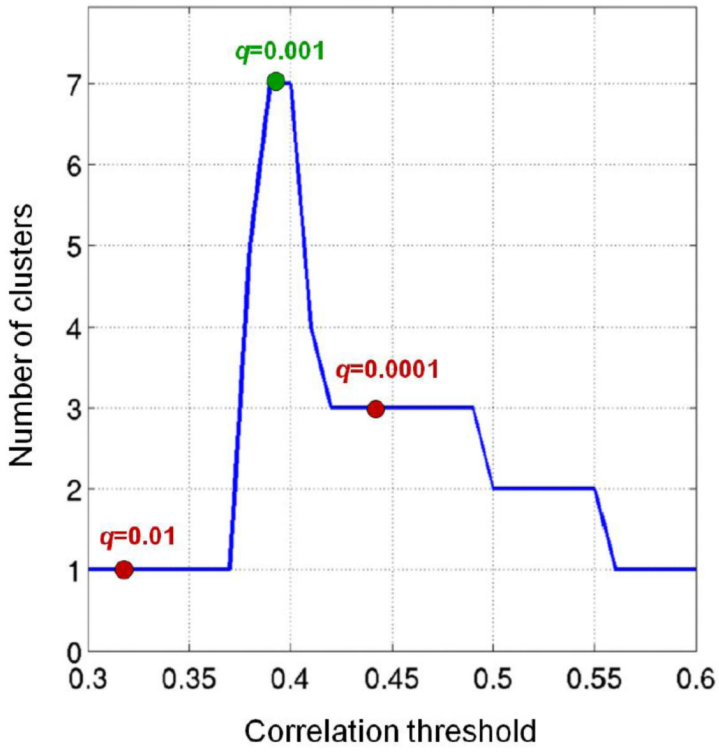

Figure 5. Analysis of correlation thresholds for the data-driven inter-species analysis

The number of clusters containing monkey and human ICs is plotted for different values of the correlation threshold (assessed between 0.3 and 0.6 at steps of 0.01). The values for correlations corresponding to an FDR of q=0.01, q=0.001 and q=0.0001 are marked with a circle. The selected configuration (FDR of q=0.001) is indicated in green, the remaining ones in red.

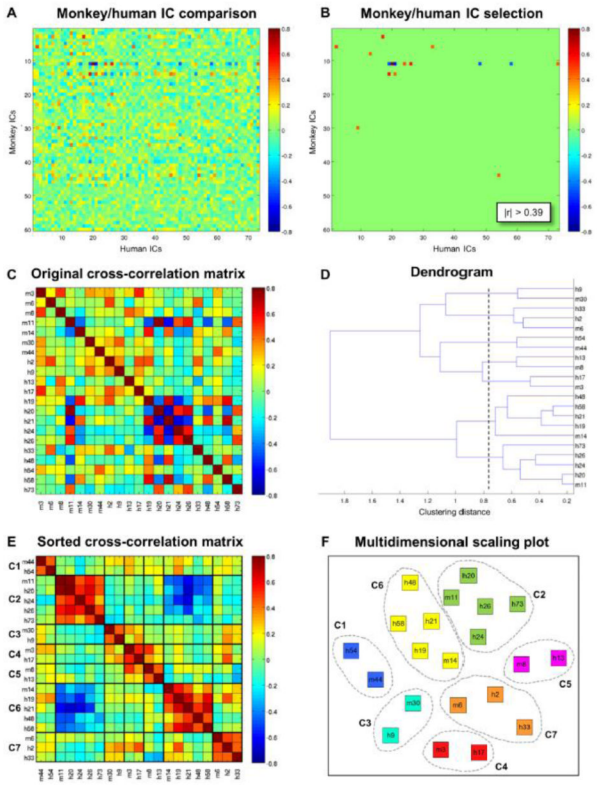

Figure 6. Clustering of monkey and human ICs with similar temporal profile

(**A**) A cross-correlation matrix is computed on the monkey and human IC timecourses. (**B**) The cross-correlation matrix is thresholded to delineate monkey and human ICs with correlated (FDR of q=0.001) timecourses. (**C**) The selected timecourses are subjected to hierarchical cluster analysis, using temporal correlation as a similarity metric. (**D**) The dendrogram is cut to delineate clusters with a least one monkey IC and one human IC. (**E**) Seven monkey-human IC clusters are defined, and the strength of the intra- and inter-cluster correlations is assessed. (**F**) Two-dimensional multidimensional scaling (MDS) plot for the seven monkey-human IC clusters. The ICs belonging to the same cluster are labeled with the same color.

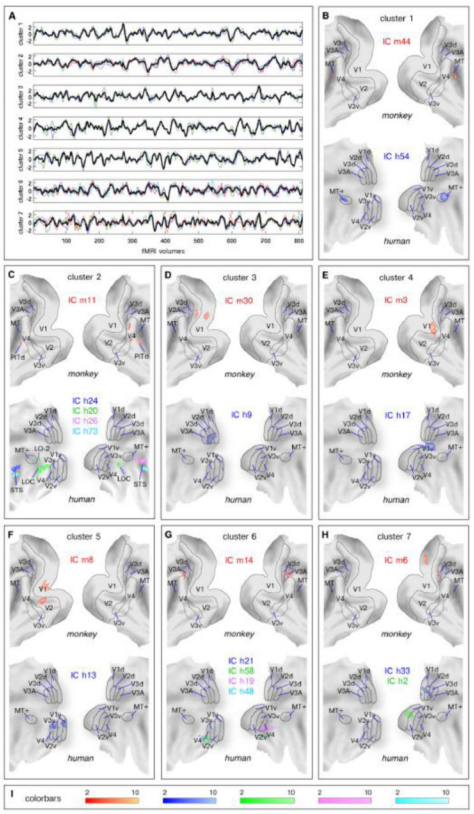

Figure 7. Timecourses and spatial maps of monkey-human IC clusters

(**A**) For each of the 7 clusters, the timecourses of the constituent monkey and human IC are plotted in different colors, whereas their average (representative of the whole cluster) is indicated by a thick black line. (**B-H**) Monkey and human IC spatial maps in each of the 7 clusters are represented (Z>2) in different colors on a flattened monkey and human cortex, respectively. The IC labels (e.g., IC m44 and IC h54 for cluster 1) correspond to the numbers of the IC clusters retrieved from monkey and human data, respectively. (**I**) Colorbars illustrating the relationship between the colors and the value range in the flat maps.

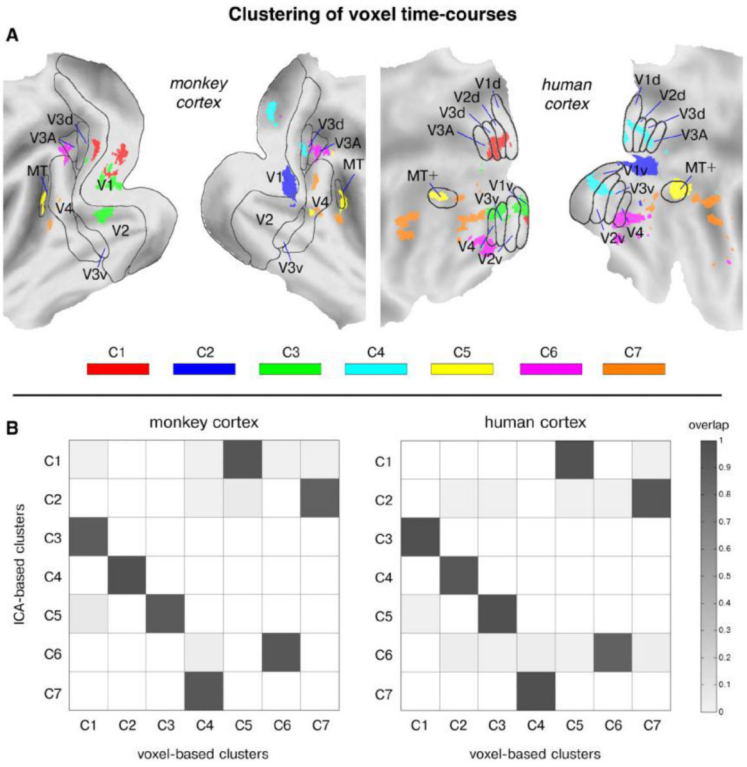

Figure 8. Clustering of timecourses from voxels belonging to selected monkey and human ICs

We extracted fMRI timecourses from the voxels included in the monkey and human ICs showing significant inter-species activity correlation (shown in Fig. 7B-H). Next, we performed a hierarchical cluster analysis on them, to define 7 clusters as in the inter-species ICA-based analysis (see Supplementary Fig. 2). (**A**) The voxel-based clusters are spatially represented with different color code over a monkey and a human flattened cortex. (**B**) We measured the spatial overlap between the seven ICA-based clusters (Fig. 7B-H) and the seven voxel-based clusters (Fig. 8A), separately for the monkey and human maps.

Table 1

Analysis of monkey and human eye data during natural vision

Saccade rate (in units/minute) and eye-position variability (in visual degrees) are provided for monkeys and humans, respectively. Eye-position overlap (expressed in percentage over time) and eye-gaze synchronization (measured by temporal correlation) are provided not only for the two species separately, but also between species.

	saccade rate	eye-position variability	eye-position overlap	eye-gaze synchronization
monkeys	11.9±0.8	2.58±0.09	64.9±1.1	0.36±0.01
humans	16.6±1.9	3.06±0.18	54.3±2.9	0.25±0.02
monkey/human	–	–	55.7±1.7	0.22

Table 2

Temporal correlation between the IC cluster timecourses and reference timecourses related to movie motion, monkey eye speed and human eye speed, respectively. Significant correlation values ($P<0.01$) are in bold.

	Movie motion	Monkey eye speed	Human eye speed
IC cluster 1	**r=0.53, *P*<0.001**	**r=0.46, *P*<0.001**	**r=0.38, *P*<0.001**
IC cluster 2	r=−0.07, *P*=0.457	r=−0.07, *P*=0.453	r=−0.03, *P*=0.750
IC cluster 3	**r=0.25, *P*=0.007**	r=0.11, *P*=0.242	r=0.02, *P*=0.832
IC cluster 4	**r=0.28, *P*=0.002**	r=0.19, *P*=0.042	r=0.19, *P*=0.040
IC cluster 5	r=0.03, *P*=0.747	r=0.02, *P*=0.827	r=0.01, *P*=0.915
IC cluster 6	r=0.20, *P*=0.032	**r=0.33, *P*<0.001**	**r=0.27, *P*=0.004**
IC cluster 7	**r=0.38, *P*<0.001**	r=0.23, *P*=0.018	r=0.18, *P*=0.054